THE JOURNAL OF PROSTHETIC DENTISTRY

RESEARCH AND EDUCATION

In vitro evaluation of the shear bond strength and bioactivity of a bioceramic cement for bonding monolithic zirconia

Chrysoula Dandoulaki, DDS,[a] Athanasios E. Rigos, DDS,[b] Eleana Kontonasaki, DDS, MSc, PhD,[c] Vassilis Karagiannis, PhD,[d] Maria Kokoti, DDS, PhD,[e] Georgios S. Theodorou, BSc, PhD,[f] Lambrini Papadopoulou, BSc, PhD,[g] and Petros Koidis, DDS, MS, PhD[h]

ABSTRACT

Statement of problem. Adhesive cementation is the most common bonding strategy for zirconia restorations. Although cementation with a bioactive luting agent has been proposed as an alternative, how the bond strength compares is unclear.

Purpose. The purpose of this in vitro study was to evaluate shear bond strength after cementing a monolithic zirconia ceramic to human dentin with a bioceramic cement, compare it with a traditional cement, and evaluate its bioactive properties.

Material and methods. A total of 120 dentin specimens and 120 yttria-stabilized tetragonal zirconia polycrystal (Y-TZP) (BruxZir) cylindrical specimens were used. Zirconia and dentin specimens were randomly divided into 8 study groups (n=15) based on 2 luting cement types (a bioceramic cement or glass ionomer cement as control), 2 airborne-particle abrasion protocols (50 μm or 110 μm), and 2 water storage durations (24 hours or 30 days). After the shear bond strength test using a universal machine at a crosshead speed of 1 mm/min, fracture patterns were evaluated under a stereomicroscope and a scanning electron microscope. Strength values were statistically analyzed with a 3-factor ANOVA model (α=.05). Bioactivity was evaluated in simulated body fluid (SBF).

Results. The control glass ionomer cement achieved significantly greater shear bond strength compared with the tested bioceramic cement. Mean bond strength values ranged from 2.52 MPa to 5.23 MPa for the bioceramic cement tested and from 4.20 MPa to 6.61 MPa for the control cement. The duration of water storage played a significant role in the bond strength, with groups stored for 30 days reaching higher bond strength values, whereas the particle size of airborne-particle abrasion did not have a significant effect. Failure types were primarily mixed. No apatite formation was recorded on the surface of the specimens even after 30 days of immersion in SBF.

Conclusions. The evaluated cement did not develop apatite in SBF, and its bond strength values were below the control glass ionomer cement. (J Prosthet Dent 2019;122:167.e1-e10)

Dental zirconia has attracted considerable interest as a restorative material. However, the issue of zirconia cementation remains a challenge, and both adhesive and nonadhesive luting cements have been proposed.[1,2] Most in vitro studies have concluded that composite resin cements provide a stronger bond between zirconia ceramics and dentin.[1,3-5] However, the clinical environment varies significantly from in vitro experimental conditions, and bond strength is not the ultimate factor affecting the selection of a luting cement. Subgingival margins, situations in which moisture control is unattainable, individuals with a high risk of caries, and unpredictable patient factors can make nonadhesive cements an alternative to adhesive cements, despite their lower bond

[a]Postgraduate student, Laboratory of Prosthodontics, Department of Dentistry, Faculty of Health Sciences, Aristotle University of Thessaloniki, Thessaloniki, Greece.
[b]Private practice, Cambridge, United Kingdom.
[c]Assistant Professor, Laboratory of Prosthodontics, Department of Dentistry, Faculty of Health Sciences, Aristotle University of Thessaloniki, Thessaloniki, Greece.
[d]Research Personnel, Statistics and Operational Research Department, School of Mathematics, Faculty of Sciences, Aristotle University of Thessaloniki, Thessaloniki, Greece.
[e]Assistant Professor, Laboratory of Prosthodontics, Department of Dentistry, Faculty of Health Sciences, Aristotle University of Thessaloniki, Thessaloniki, Greece.
[f]Postdoctoral Researcher, Physics Department, Faculty of Sciences, Aristotle University of Thessaloniki, Thessaloniki, Greece.
[g]Assistant Professor, Geology Department, Faculty of Sciences, Aristotle University of Thessaloniki, Thessaloniki, Greece.
[h]Professor and Head, Laboratory of Prosthodontics, Department of Dentistry, Faculty of Health Sciences, Aristotle University of Thessaloniki, Thessaloniki, Greece.

Clinical Implications

Given the limitations of this in vitro study, the studied bioceramic cement is not indicated for the cementation of monolithic zirconia restorations because of its relatively low bond strength. In addition, the lack of apatite formation does not support any clinical benefit of using this cement type.

strength.[2] For retentive tooth preparations, conventional nonadhesive luting agents have been considered appropriate[6] despite the lack of a chemical bond between the cement and the zirconia surface.

Ceramir C&B (Doxa Dental Inc) is a nonresin cement recommended for cementing monolithic zirconia restorations, which, according to the manufacturers, belongs to a new class of biomaterials, the nanostructurally integrating bioceramics (NIB). This cement is based on calcium aluminate and glass ionomer components and has been suggested to have bioactive properties.[7] The concept relies on the potential for remineralizing the tooth structure of the release of Ca^{2+} and PO_4^{2-} and the formation of hydroxyapatite (HAp).[8,9] This could reduce the incidence of secondary caries and postoperative sensitivity as its bioactive properties could protect the marginal seal of the restoration.[10] The authors are aware of only a single in vitro study reporting that after 7 days of immersion in saliva and Dulbecco D 8662 phosphate-buffered saline (PBS), a HAp phase developed on the surfaces of the immersed specimens.[11] The presence of high amounts of phosphorous in the PBS in addition to the phosphorous from the cement was responsible for the layer that developed. However, documentation concerning its apatite-forming ability in SBF is lacking, which is the gold standard for testing bioactive materials,[12] although it contains a significantly lower amount of phosphorous compared with PBS or simulated dentinal fluid (SDF).[13,14] Glass ionomer cements are incapable of promoting HAp formation[8,15] but do have good mechanical properties even after long-term water storage.[16-22]

To enhance the bond strength of zirconia ceramics to cement, various surface treatments have been proposed, including airborne-particle abrasion (APA) and tribochemical silica coating (TBC).[23-36] APA improves bond strength through micromechanical interlocking,[6] and TBC improves bond strength through a combination of surface roughening and chemical bonding.[29]

Shear bond strength (SBS) and tensile bond strength (TBS) tests have been used to evaluate the bond strength of different ceramic materials.[37] The use of micro-SBS tests and micro-TBS tests have been suggested to minimize the critical flaws in the cement mass that can cause failure of the bond.[38] The SBS tests, with a bonding area of less than 3 mm^2, minimize the critical flaws concentrated in the cement mass[38] and the stress concentration near the loading site.[37]

The purpose of this in vitro study was to investigate the apatite-forming ability of a bioceramic cement and to evaluate its SBS for bonding monolithic zirconia to human dentin compared with a GIC after zirconia APA with 2 different Al_2O_3 particle sizes and postcementation water storage (WS). The null hypotheses were that the luting cement type, APA particle size, and WS duration would not influence the bond strength of monolithic zirconia to human dentin.

MATERIAL AND METHODS

Sixty freshly extracted, intact fully erupted human third molars were collected according to the guidelines of the Institutional Ethics Committee, cleaned of organic remnants, and stored in 1% aqueous chloramine-T solution at 4 °C according to ISO 29022:2013. The roots were resected, and the crown was sectioned in the mesiodistal dimension in order for each buccal and lingual half to result in a separate specimen.[39,40] The buccal or lingual surface of each half resulted in 1 dentin specimen after wet grinding the enamel surface until a cementation area was exposed exclusively on the superficial dentin. The dentin cementation surface was placed inside a cylinder mold facing the base, which was then poured with autopolymerizing acrylic resin (Triplex; Ivoclar Vivadent AG). The dentin specimens were stored in distilled water until cementation. The dentin surface of every cylinder underwent water polishing (Ecomet III; Buehler) with 600-grit silicon carbide paper for 60 seconds to standardize the surface. The surface was evaluated under a stereomicroscope to ensure the absence of enamel. Each dentin specimen was given a number (1-120).

Blocks of monolithic zirconia (BruxZir; Lot #BZ1226283 Solid Zirconia) were used to produce specimens with final dimensions of 1.8 mm in diameter and 2 mm in height after sintering. The surface to be cemented underwent water polishing (Ecomet III; Buehler) with 800-, 1000-, and 1200-grit silicon carbide paper for 60 seconds. Polished surfaces were inspected under a stereomicroscope to secure homogenous surfaces, and specimens were ultrasonically cleaned (Branson 200; Branson Ultrasonics Corp) in isopropyl alcohol. Zirconia surface conditioning was performed perpendicularly to the cementation surface with 50-μm or 110-μm Al_2O_3 particles (APA50, APA110) for 10 seconds from a distance of 10 mm with 300 kPa pressure. The specimens were cleaned ultrasonically in isopropyl alcohol and dried in air. Zirconia and dentin specimens were randomly divided into 8 groups (Fig. 1) based on 2 cement types

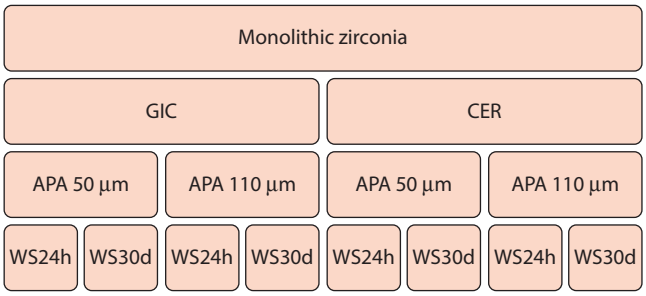

Figure 1. Study groups according to cement type, zirconia surface conditioning, and storage before shear bond strength (SBS) test. APA, airborne-particle abrasion; CER, ceramir; GIC, glass ionomer cement; WS, water storage.

(bioceramic [CER-Ceramir C&B; Doxa Dental AB; Lot #101777] or glass ionomer cement [GIC- GC Fuji I; Lot #170215A; GC Corp]), 2 airborne-particle abrasion protocols (APA50, APA110), and 2 water storage durations (24 hours [WS24h] or 30 days [WS30d]). The assignment of the 120 specimens to each group was performed through random block allocation (www.randomizer.org). A conventional GIC based on calcium aluminofluorosilicate glass was selected as a control because of its compositional affinity with the tested cement, which is based on a SiO_2-Al_2O_3-SrO-P_2O_5-NaO_2-F–glass and calcium aluminate. The manufacturer instructions were followed, and the specimens were placed in a custom-made bonding clamp to standardize the loading force until the removal of the excess cement.[39,41] All procedures were performed by the same operator (C.D.) to minimize variability.

After WS, the cemented specimens were placed in a universal testing machine (Testometric M350-10CT; The Testometric Co Ltd) for the shear bond strength (SBS) test. Load until fracture was applied at a crosshead speed of 1 mm/min. SBS values were calculated by using the formula P/A, where P is the force at fracture (N) and A is the bonded area in mm^2.[39] The fractographic analysis included an initial evaluation under a stereomicroscope (Stemi DV4; Zeiss) at ×40 magnification. The modes of failure were classified as follows: cohesive, where more than two thirds of the zirconia surface and the dentin surface appeared to be covered by cement remnants; adhesive at the ceramic-cement interface (adhesive-Zir), where less than one third of the debonded zirconia surface presented cement remnants; adhesive at the dentin-cement interface (adhesive-D), where less than one third of the debonded dentin surface presented cement remnants; and mixed, where a combination of adhesive and cohesive failures was detected. Debonded specimens were evaluated with scanning electron microscopy (SEM)–energy-dispersive X-ray spectroscopy (SEM-EDS) (JEOL JSM 840A; JEOL).

The assumptions of normality and equality of variances of the SBS values for each combination of cement, APA, and WS were studied with the Shapiro-Wilk and Levene tests and were initially rejected. According to the Tukey spread-versus-level plot, the data were transformed with the natural log function. Cochran's test[42] revealed that the distributions of the Ln [SBS (MPa)] had outlying variances in 4 occasions, CER-APA50-WS30d, GIC-APA110-WS24h, CER-APA50-WS24h, and CER-APA110-WS24h (Fig. 2B). Applying Dixon's and Grubbs' tests[43-46] to all groups, 4 specimens with the lowest values (Fig. 2B) were characterized as outliers and were removed. These tests were performed with the package "outliers," Version 0.14[42] in the statistical software R version 3.3.1 (http://www.r-project.org). After removal of the 4 specimens, the assumptions were met. As a result, the data were statistically analyzed with the 3-way ANOVA. However, as the 3-way interaction term and the 2-way interactions terms were not statistically significant, the final model was based on main effects. The analysis of variance models was conducted with statistical software (IBM SPSS Statistics, v21.0; IBM Corp).[47] For the failure mode analysis, the Pearson chi-square test was used, but the results were not valid because of the 66.7% of cells with expected counts of less than 5 and 30% less than one. Accordingly, an unbiased estimate of the exact significance level was calculated with the Monte Carlo method based on 100 000 tables from the data. The upper bound of the 99% confidence interval for the exact P value was .00046, verifying the result of the asymptotic P value (α=.05 for all tests).

For the apatite-forming ability testing, disk-shaped specimens of CER were fabricated by using the following procedure: capsules were mixed (Rotomix; 3M ESPE) for 8 seconds, and polyvinylsiloxane silicone (Kulzer Variotime easy putty; Kulzer GmbH) molds (3 mm in diameter × 1 mm in height) were filled with the cement. After initial hardening, the specimens were kept in double-distilled water for 3 hours at 37 °C for complete setting. A total of 24 specimens were fabricated. The SBF (c-SBF) was prepared according to a previous study.[48] Three specimens were not immersed and served as control. Three specimens for each time period were kept in 15 mL (surface area-to-volume ratio=0.1 cm^{-1})[48] SBF (1, 4, 8, 12, 18, 30 days) and three in 15 mL double-distilled water for 30 days. All specimens were kept in an incubator at 37 °C under static conditions. After each time point, the specimens were removed from the solution, thoroughly washed with double-distilled water, and air-dried. For structural and morphological characterization, the specimens were analyzed by Fourier transform infrared spectroscopy (FTIR), X-ray diffraction analysis (XRD), and SEM-EDS.[49-54] FTIR transmittance spectra were obtained in the mid-infrared (MIR) region with a resolution of 4 cm^{-1} by using the KBr pellet technique. XRD analysis was performed with the Bragg–Brentano geometry,[55]

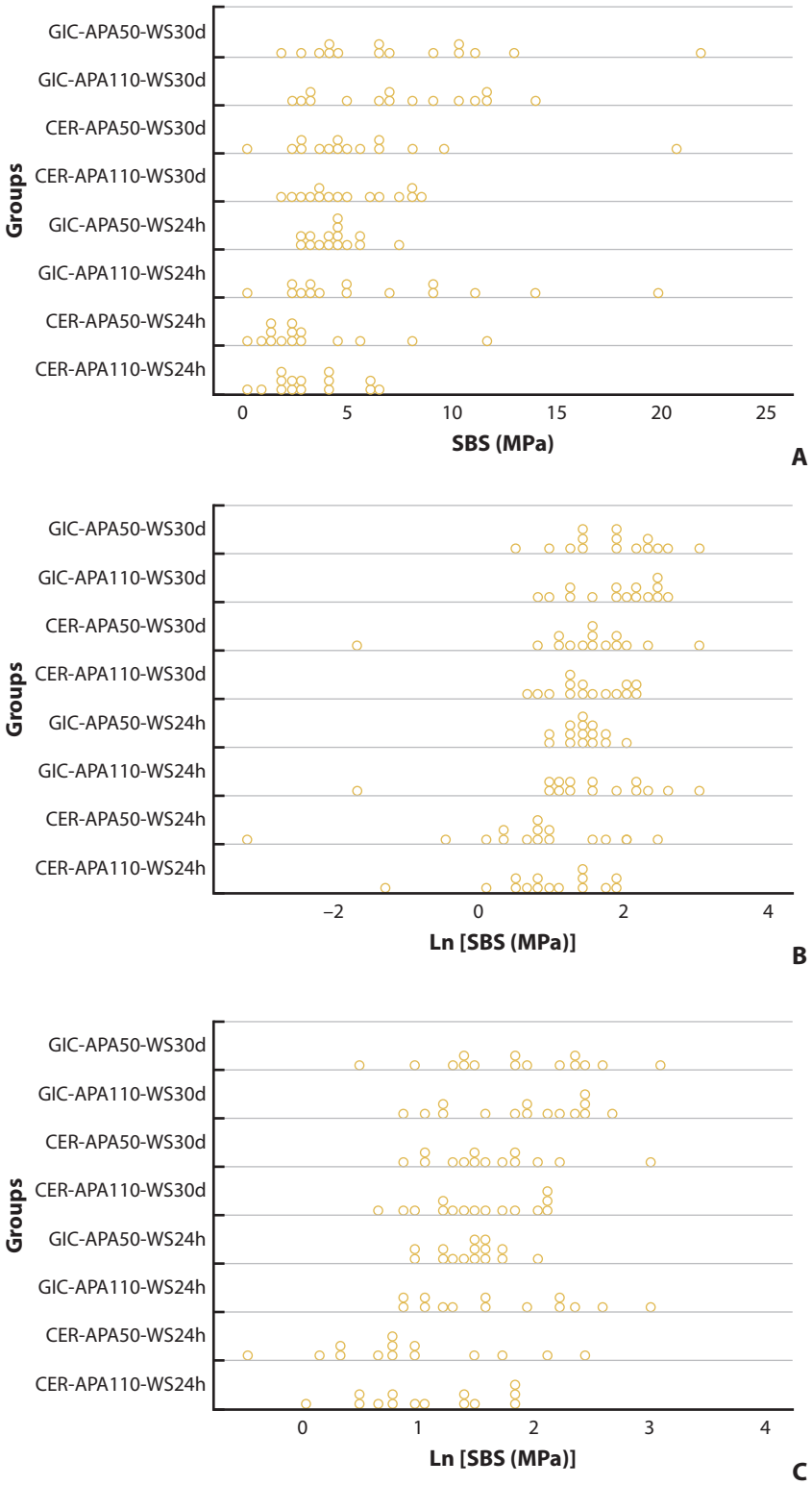

Figure 2. Distribution of shear bond strength (SBS) values. A, Data from all specimens. B, Log-transformed data from all specimens. C, Log-transformed data after exclusion of 4 specimens. APA, airborne-particle abrasion; CER, ceramir; GIC, glass ionomer cement; WS, water storage.

with CuKα radiation in the range (2θ): 5-75 degrees. The parameters set were as follows: step size, 0.02 degrees 2θ; count step, 2.5 sec/step. For SEM-EDS, the specimens were carbon-coated, and surface morphological and elemental analysis was performed at various magnifications.

Table 1. Descriptive statistics for each combination of study factors

Groups	N	Min	Max	Median	Mean ±SD	Geometric Mean	Geometric SD	CV (%) Log (SBS)
CER-APA110-WS24h	14	1.03	6.44	2.73	3.38 ±1.85	2.91	1.78	53.8
CER-APA110-WS30d	15	2	8.52	4.41	5.02 ±2.25	4.53	1.61	31.5
CER-APA50-WS24h	14	0.62	11.48	2.18	3.42 ±3.06	2.52	2.20	85.0
CER-APA50-WS30d	14	2.34	20.79	4.78	6.20 ±4.66	5.23	1.75	33.9
GIC-APA110-WS24h	14	2.47	19.92	4.9	6.99 ±5.16	5.58	1.98	39.8
GIC-APA110-WS30d	15	2.34	14.11	7.18	7.59 ±3.74	6.61	1.78	30.6
GIC-APA50-WS24h	15	2.62	7.43	4.33	4.36 ±1.26	4.20	1.33	19.8
GIC-APA50-WS30d	15	1.69	21.93	6.55	7.7 ±5.20	6.29	1.97	36.8

APA, airborne-particle abrasion; CER, ceramir; GIC, glass ionomer cement; SD, standard deviation; WS, water storage.

Table 2. Results of 3-way ANOVA

Source	Type III Sum of Squares	df	Mean Square	F	*P*	Partial Eta Squared
Corrected model	12.243	7	1.749	4.986	<.001	0.244
Intercept	262.532	1	262.532	748.409	<.001	0.874
Cement type	5.358	1	5.358	15.275	<.001	0.124
APA grain size	0.203	1	0.203	0.578	.449	0.005
WS duration	5.501	1	5.501	15.681	<.001	0.127
Cement type×APA grain size	0.198	1	0.198	0.563	.454	0.005
Cement type×WS duration	0.644	1	0.644	1.835	.178	0.017
APA grain size×WS duration	0.489	1	0.489	1.393	.241	0.013
Cement type×APA grain size×WS duration	0.005	1	0.005	0.014	.906	0
Error	37.885	108	0.351			
Total	314.944	116				
Corrected total	50.128	115				

APA, airborne-particle abrasion; WS, water storage.

Table 3. Tests of between-subject effects from 3-way ANOVA without 3-way interaction term R squared=0.244; adjusted R squared=0.203

Source	Type III Sum of Squares	df	Mean Square	F	*P*	Partial Eta Squared
Corrected model	12.238	6	2.040	5.868	<.001	.244
Intercept	262.532	1	262.532	755.240	<.001	.874
Cement type	5.365	1	5.365	15.435	<.001	.124
APA grain size	0.203	1	.203	.584	.447	.005
WS duration	5.497	1	5.497	15.812	<.001	.127
Cement type×APA grain size	0.199	1	.199	.572	.451	.005
Cement type×WS duration	0.644	1	.644	1.852	.176	.017
APA grain size×WS duration	0.487	1	.487	1.401	.239	.013
Error	37.890	109	.348			
Total	314.944	116				
Corrected total	50.128	115				

APA, airborne-particle abrasion; WS, water storage.

RESULTS

The dot plot (Fig. 2A) shows that the distributions of the SBS values were positively skewed with unequal variances, which was also verified by the Shapiro-Wilk test of normality and the Levene test of equality of variances. The Cochran test for outlying variance and the Dixon and Grubbs tests for outliers revealed that the 4 observations with the lowest values in Figure 2B should be removed. After removal of these specimens, the assumptions of normality and equality of variances of Ln(SBS [MPa]) for each of the 8 groups in Figure 2C were not rejected. Descriptive statistics for the final sample are presented in Table 1. Based on the aforementioned exploratory data analysis, the natural log SBS, Ln(SBS [MPa]) was used as the dependent variable (after excluding the 4 specimens). Initially, a 3-way ANOVA was performed and revealed a nonsignificant 3-way interaction term (F[1108]=0.014, *P*=.906, Table 2). The analysis was rerun without the 3-way interaction term, and the results showed that neither of the 2-way interaction terms was significant [(Cement type)×(APA grain size), F(1,109)=0.572, *P*=.451, (Cement type)×(WS duration), F(1,109) =1.852, *P*=.176 and (APA grain size)×(WS duration), F(1,109)=1.401, *P*=.239] (Table 3). Consequently, the final analysis was performed with the main effect 3-way ANOVA model. The results revealed that both main effects of cement (F(1,112)=15.160, *P*<.001, partial eta squared=11.9%) and WS (F(1,112)=15.534, *P*<.001, partial eta squared=12.2%) were statistically significant (Table 4). Specifically, the effect of GIC (antilog-transformed estimated marginal mean=5.57, 95% confidence interval [CI]: 4.78-6.49) was 1.53 (95% CI: 1.23-1.91) times greater than the effect of CER (antilog-transformed estimated marginal mean=3.63, 95% CI: 3.11-4.24), and the effect of 30 days (antilog-transformed estimated marginal mean=5.58, 95% CI: 4.79-6.51) was 1.54 (95% CI: 1.24-1.92) times greater than the effect of 24 hours (antilog-transformed estimated marginal mean=3.62, 95% CI: 3.10-4.23).

Predominantly, mixed types of failures for all groups were observed (Table 5). The failure type "mixed" is expected for all groups, the "adhesive-Zir" type is expected mainly in groups CER-APA110-WS30d and CER-APA50-WS24h, while the "Adhesive-D" type is expected only for CER-APA50-WS24h (χ^2[14]=42.552, Monte Carlo 99% CI: 0-00046). Representative SEM micrographs of the zirconia specimens before and after

Table 4. Tests of between-subject effects from main effect 3-way ANOVA (dependent variable: Ln(SBS [MPa]), R squared=0.218 [adjusted R squared=0.197])

Source	Type III Sum of Squares	df	Mean Square	F	P	Partial Eta Squared
Corrected model	10.939	3	3.646	10.422	<.001	.218
Intercept	262.065	1	262.065	748.977	<.001	.870
Cement type	5.304	1	5.304	15.160	<.001	.119
APA grain size	0.199	1	.199	.569	.452	.005
WS duration	5.435	1	5.435	15.534	<.001	.122
Error	39.188	112	.350			
Total	314.944	116				
Corrected total	50.128	115				

APA, airborne-particle abrasion; WS, water storage.

Table 5. Distribution of various failure types in each experimental group

Groups	N	Mixed (%)	Cohesive (%)	Adhesive-D (Dentin) (%)	Adhesive-Zir (Zirconia) (%)
GIC-APA50-WS24h	15	73	0	0	27
GIC-APA110-WS24h	14	50	0	0	50
GIC-APA50-WS30d	15	47	6	0	47
GIC-APA110-WS30d	15	93	0	0	7
CER-APA50-WS24h	14	100	0	0	0
CER-APA110-WS24h	14	100	0	0	0
CER-APA50-WS30d	14	100	0	0	0
CER-APA110-WS30d	15	100	0	0	0

APA, airborne-particle abrasion; CER, ceramir; GIC, glass ionomer cement; WS, water storage.

APA are presented in Figure 3. As Al_2O_3 particles increase in size, the surface becomes coarser with deeper and larger grooves. Some representative fractured zirconia specimens with their respective dentin surfaces are presented in Figure 4. A mixed failure type is presented in Figure 4A, in which dispersed areas of remaining cement on the dentin surface are evident (Fig. 4A, spectra 2,3). The white areas on the backscattered microphotograph of the zirconia specimen in Figure 4A correspond to the zirconia substrate as verified by EDS analyses (high amount of Zir in spectra 1,3), while the dark areas correspond to the remaining cement, which is rich in Al, Si, Sr, and F (spectrum 2). Similarly, a mixed type is presented in Figure 4B, in which a large area of remaining bioactive cement is observed in the center of the specimen both in the secondary electrons and the backscattered microphotograph of the zirconia specimen. As shown in the backscattered microphotograph of the zirconia specimen in Figure 4B, spectrum 1, the bioactive cement consists of F, Na, Al, Si, and a high amount of Sr. On the contrary, an adhesive-Zir type is observed in Figure 4C, as the whole dentin surface is covered by a layer of GIC (Fig. 4C). The backscattered microphotograph of the dentin specimen, spectra 1-3, and the EDS analysis performed on the backscattered

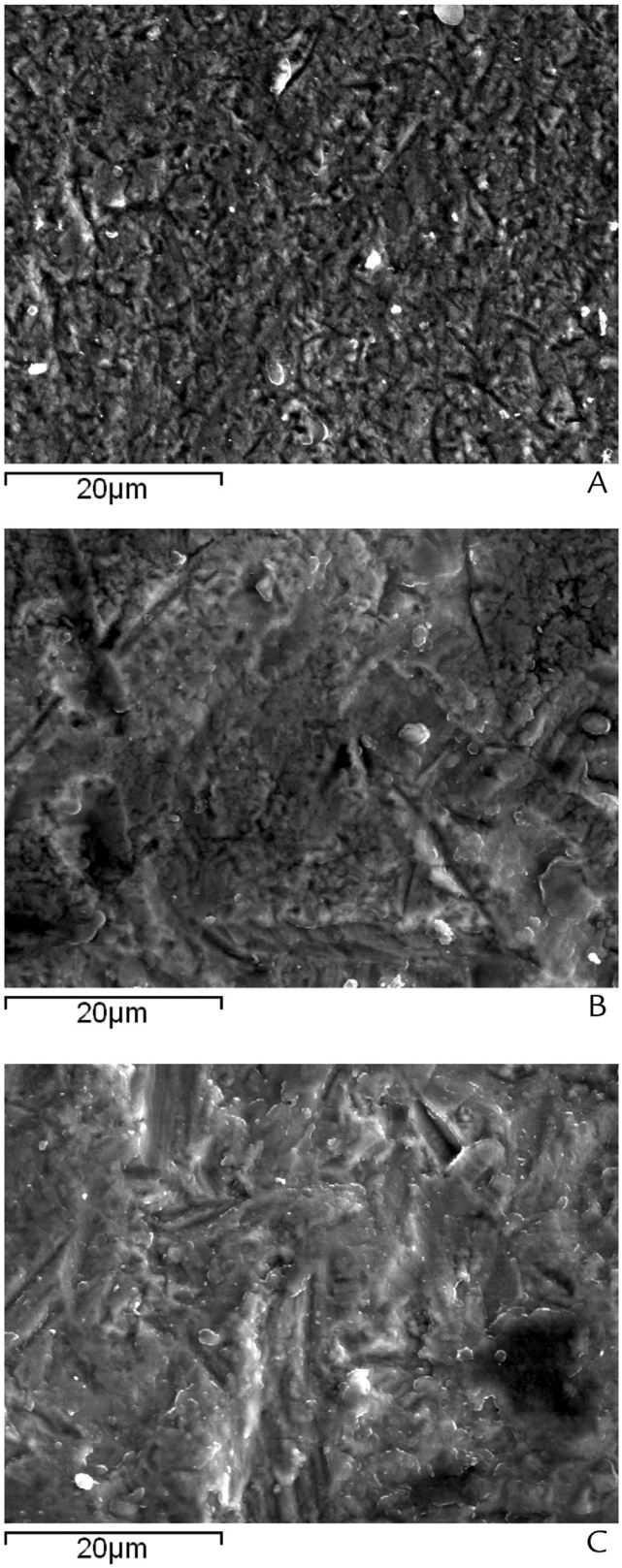

Figure 3. Scanning electron microscope images of zirconia specimens after surface treatment. A, As received. B, After airborne-particle abrasion 50 μm (APA50). C, After airborne-particle abrasion 100 μm (APA110). Original magnification ×2000.

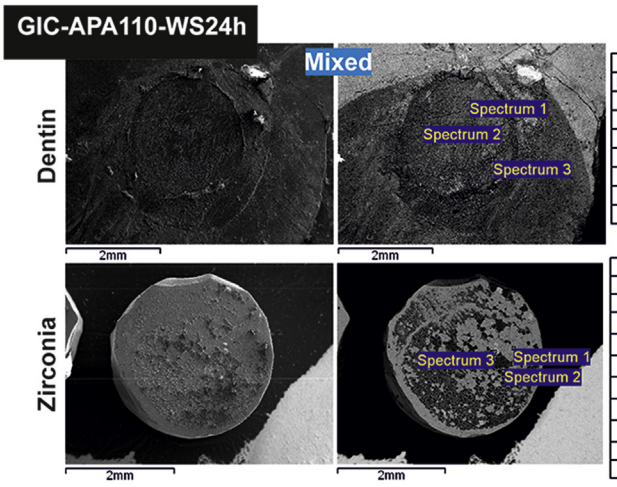

	Spectrum 1	Spectrum 2	Spectrum 3
Element	Weight%	Weight%	Weight%
Al	4,59	25,93	15,52
Si	3,33	9,55	8,3
P	13,18	1,87	4,06
Ca	28,65	5,63	7,41
Sr	11,77	15,57	28,12
O	38,48	41,45	36,59
Totals	100	100	100

	Spectrum 1	Spectrum 2	Spectrum 3
Element	Weight%	Weight%	Weight%
Al	7,18	13,42	3,44
Si	-	14,29	-
P	-	-	-
Zr	63,99	-	69,22
Sr	-	28,96	-
F	-	5,35	-
Ca	-	3,21	-
O	28,83	34,78	27,34
Totals	100	100	100

A

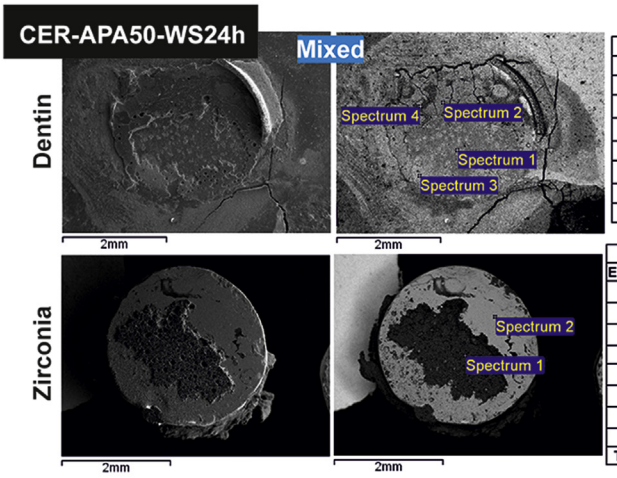

	Spectrum 1	Spectrum 2	Spectrum 3	Spectrum 4
Element	Weight%	Weight%	Weight%	Weight%
Al	4,19	21,29	24,64	49,16
Si	-	3,48	2,51	-
P	16,4	0,63	0,88	-
Ca	38,97	26,79	27,02	5,09
Sr	-	11,34	6,98	-
O	40,45	36,47	37,97	45,75
Totals	100	100	100	100

	Spectrum 1	Spectrum 2
Element	Weight%	Weight%
F	5,92	-
Na	1,24	-
Al	16,7	-
Si	11,44	1,48
Ca	5,73	-
Sr	23,98	-
Zr	-	71,68
O	34,99	26,83
Totals	100	100

B

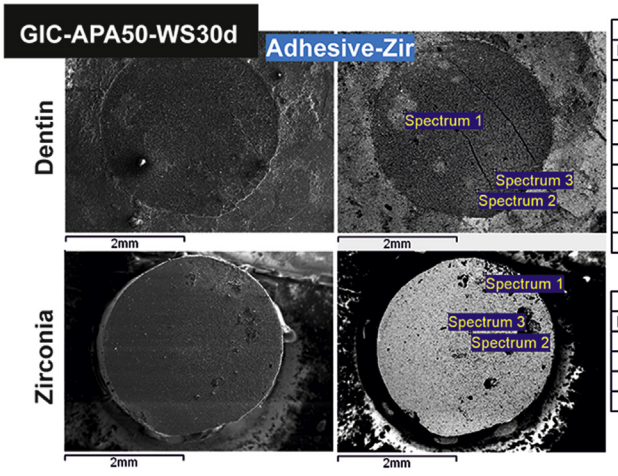

	spectrum 1	spectrum 2	spectrum 3
Element	Weight%	Weight%	Weight%
F	7,01	9,65	7,3
Al	22,86	23,39	18,65
Si	15,26	10,5	24,1
P	1,14	1,58	-
Ca	6,89	12,96	1,84
Ba	-	-	0,59
Yb	-	-	2,36
O	46,84	41,93	45,17
Totals	100	100,01	100,01

	spectrum 1	spectrum 2	spectrum 3
Element	Weight%	Weight%	Weight%
Al	0,39	2,18	3,02
Zr	73,48	70,98	69,81
O	26,12	26,84	27,17
Totals	100	100	100

C

Figure 4. Representative scanning electron microscope images of fractured interfaces. Left: microphotographs from secondary electrons; right: microphotographs from backscattered electrons. A, Dentin and zirconia surfaces of mixed-type fractured zirconia-dentin specimen subjected to airborne-particle abrasion 110 μm, cementation with glass ionomer cement (GIC), and water storage (WS) for 24 hours. B, Dentin and zirconia surfaces of mixed-type fractured zirconia-dentin specimen subjected to airborne-particle abrasion 50 μm, cementation with ceramir (CER), and water storage (WS) for 24 hours. C, Dentin and zirconia surfaces of adhesive-Zir-type fractured zirconia-dentin specimen subjected to airborne-particle abrasion 50 μm, cementation with glass ionomer cement (GIC), and water storage (WS) for 30 days. Original magnifications: A, Dentin specimen ×20; zirconia specimen ×23. B, Dentin specimen ×22; zirconia specimen ×23. C, Dentin and zirconia specimens ×25.

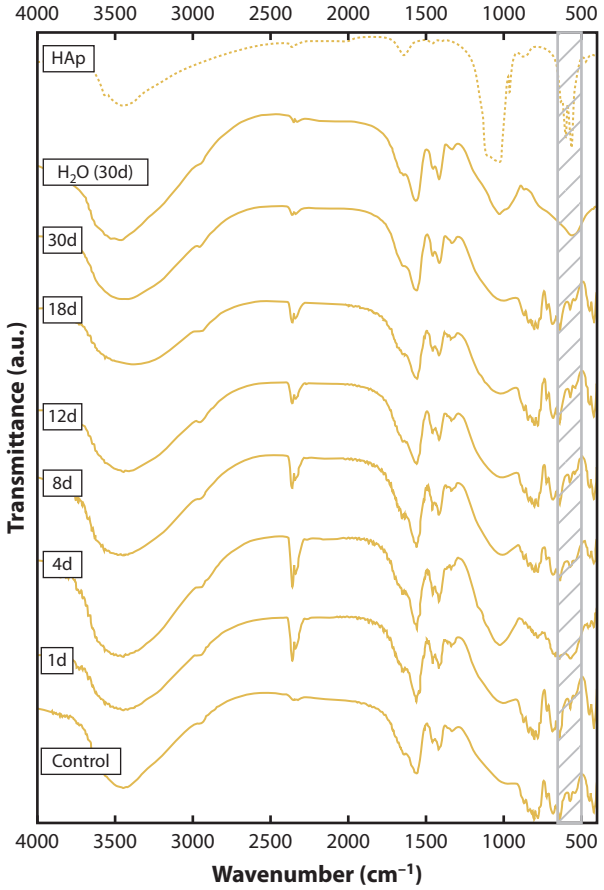

Figure 5. FTIR spectra of representative specimens before and after immersion in simulated body fluid (SBF) solution (up to 30 days) and water (after 30 days).

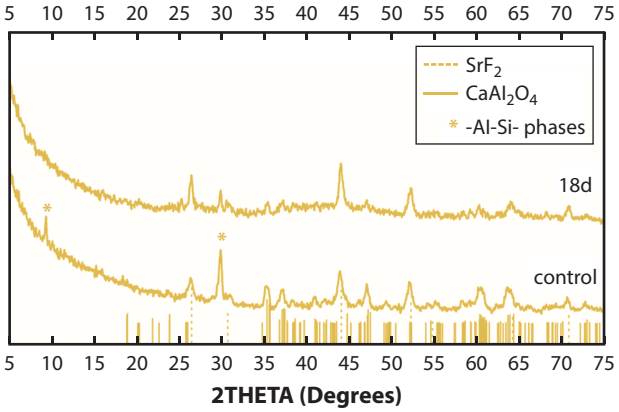

Figure 6. XRD patterns of representative specimens before and after immersion in simulated body fluid (SBF) solution for 18 days.

microphotograph of the zirconia specimen reveal only areas rich in Zir and Al from the airborne-particle abrasion (Fig. 4C, backscattered microphotograph of the zirconia specimen, spectra 1-3).

The FTIR spectrum of a representative control specimen (Fig. 5) indicates the presence of calcium aluminum oxide (CA, $CaAl_2O_4$). The peaks at 418, 448, 542, and 573 cm^{-1} are associated with the vibrational bending of AlO_4^{5-}, whereas the peaks at 684, 722, 764, 780, 788, 804, 820, 840, and 870 cm^{-1} are attributed to the vibrational stretching of AlO_4^{5-}.[49] Moreover, the peaks at 1412 and 1568 cm^{-1} are attributed to the symmetric and antisymmetric stretching frequencies of the carboxylate ion (COO-). In contrast, the peak at 1456 cm^{-1} is attributed to the CH_2 vibrational stretching and the shoulder at 1646 cm^{-1} to deformation vibrations of C-OH, all corresponding to the presence of the polymerization products of poly(acrylic acid).[52-54] The XRD patterns are in agreement with the FTIR spectra concerning the presence of CA as shown in Figure 6. XRD measurements revealed the presence of strontium fluoride (SrF_2) and of an Al-Si phase as indicated in Figure 6, but due to the complex nature of the specimen, it was not possible to identify the exact chemical formula. FTIR spectra could not assist in the identification because of the possible overlapping of multiple peaks in the 400-900 cm^{-1} area, leaving only the broad peak at ~990 cm^{-1}, probably assigned to the vibration of a Si-Al phase (SA).[56] After soaking in SBF, FTIR reveals no significant alteration even after 30 days and no HAp formation. The spectra of the specimens immersed in water for 30 days indicate that the crystalline structure of the material has deteriorated, thus depicting amorphous behavior. The XRD pattern of the specimens after immersion in SBF for 18 days does not show significant alterations and is therefore in agreement with the FTIR findings. The only difference was the peaks of SrF_2 that were more intense in comparison with the specimens before immersion in SBF.

DISCUSSION

The bond strength values achieved in the present study were significantly lower than those achieved by adhesive composite resin cements, and specimens cemented with GIC exhibited 1.55 times greater SBS compared with those cemented with CER. Failure analysis revealed that while all CER groups exhibited exclusively mixed types of failure, GIC groups presented mixed and adhesive failures at the cement-ceramic interface. This could indicate that GIC achieves a stronger bond with dentin compared with CER. Mixed failure type likely indicates a failure of the cement to achieve high bond strength to both the ceramic surface and the dentin substrate. GIC presented higher SBS values after WS for 30 days, which agrees with the results of Turker et al,[4] regardless of the APA grain size. The same was observed for the CER groups. It has already been experimentally demonstrated that GIC materials present mechanical modifications in the long term when exposed to water.[15] Their hardness tends to increase,[15] although there is no certain characteristic alteration in strength.[16,17] An increase in strength has

been correlated with the increase in the hydration of the metal-carboxylate links[18] along with a slow reaction of residual carboxylic groups with bivalent or trivalent cations.[19] After 24 hours of WS, the GIC has not achieved its highest degree of maturation and consequently attains low values of bond strength, but when sufficient time is given for complete maturation, higher bond strength can be achieved.[22] However, prolonged aging has been linked to lower bond strength values due to shrinkage and bond hydrolysis.[21] CER, as a calcium aluminate cement, sets through a combined process of dissolution and precipitation. CER, as a hybrid cement,[10] consists of glass ionomer and a calcium aluminate ceramic belonging to the same group as calcium phosphates and silicates and thus is expected to have similar properties to glass ionomer cement. Its higher SBS values after WS for 30 days could be partially attributed to its composition.

The authors are unaware of studies evaluating the in vitro SBS of this bioceramic cement. Nonetheless, according to Engqvist et al,[9] calcium aluminate cements can provide a "tight bond" to tooth tissue. However, in the present study, the bioactive potential of this cement could not be verified under the experimental conditions. Although apatite-forming ability after immersion in SBF is considered evidence of bioactivity, no HAp or other calcium phosphate phase developed on the specimen surfaces was maintained for 30 days. This may be attributed to the 10 times lower phosphorous content compared with PBS. Although dentinal fluid contains even higher amounts of phosphorous, whether its slow flow rate is adequate to engage HAp precipitation is questionable. A protocol to investigate the mineralization potential of this cement based on SDF may lead to more reliable results. Possible future clinical research may lead to different outcomes regarding its bioactive potential.

The finding of the present study that particle size for APA plays an insignificant role on SBS is consistent with those of previous publications. Although increased particle size leads to increased surface roughness for zirconia ceramics, the surface wettability and micromechanical retention does not follow that pattern when it comes to adhesive cementation.[4,23-26,31] The propulsion pressure of 300 kPa was selected as it does not cause crucial flaws that could compromise resistance.[32,34,35]

Limitations of this study include that the teeth used were of unspecified age, which may have influenced bond strength. Thermocycling would offer a more representative simulation of the oral environment compared with WS; however, it can be assumed that it would result in even lower values. Finally, the design and geometry of the SBS test have low relevance for the actual stresses in clinical situations.[37] Future investigations should include assessment with the cementation of crowns or fixed partial dentures.

CONCLUSIONS

Based on the findings of this in vitro study, the following conclusions were drawn:

1. The evaluated cement did not develop apatite in SBF, and attributed bond strength values were lower compared with the control glass ionomer cement.
2. APA grain size did not affect the bond strength, which was significantly higher after water storage.

REFERENCES

1. Ernst CP, Cohnen U, Stender E, Willershausen B. In vitro retentive strength of zirconium oxide ceramic crowns using different luting agents. J Prosthet Dent 2005;93:551-8.
2. Blatz MB, Vonderheide M, Conejo J. The effect of resin bonding on long-term success of high-strength ceramics. J Dent Res 2018;97:132-9.
3. Prylinska-Czyzewska A, Piotrowski P, Prylinski M, Dorocka-Bobkowska B. Various cements and their effects on bond strength of zirconia ceramic to enamel and dentin. Int J Prosthodont 2015;28:279-81.
4. Turker SB, Ozcan M, Mandali G, Damla I, Bugurman B, Valandro LF. Bond strength and stability of 3 luting systems on a zirconia-dentin complex. Gen Dent 2013;61:e10-3.
5. Uo M, Sjögren G, Sundh A, Goto M, Watari F, Bergman M. Effect of surface condition of dental zirconia ceramic (Denzir) on bonding. Dent Mater J 2006;25:626-31.
6. Thompson JY, Stoner BR, Piascik JR, Smith R. Adhesion/cementation to zirconia and other non-silicate ceramics: Where are we now? Dent Mater 2011;27:71-82.
7. Ceramir Crown & Bridge. How to use & indications [Internet]. Available at: http://ceramirus.com/how-to-indication/. Accessed January 31, 2019.
8. Lööf J, Svahn F, Jarmar T, Engqvist H, Pameijer CH. A comparative study of the bioactivity of three materials for dental applications. Dent Mater 2008;24:653-9.
9. Engqvist H, Schultz-Walz JE, Loof J, Botton GA, Mayer D, Phaneuf MW, et al. Chemical and biological integration of a mouldable bioactive ceramic material capable of forming apatite in vivo in teeth. Biomaterials 2004;25:2781-7.
10. Jefferies SR, Pameijer CH, Appleby DC, Boston D, Galbraith C, Lööf J, et al. Prospective observation of a new bioactive luting cement: 2-year follow-up. J Prosthodont 2012;21:33-41.
11. Engstrand J, Unosson E, Engqvist H. Hydroxyapatite formation on a novel dental cement in human saliva. ISRN Dent 2012;2012:1-7.
12. Kokubo T, Yamaguchi S. Novel bioactive materials developed by simulated body fluid evaluation: Surface-modified Ti metal and its alloys. Acta Biomater 2016;44:16-30.
13. Özok AR, Wu MK, Ten Cate JM, Wesselink PR. Effect of dentinal fluid composition on dentin demineralization in vitro. J Dent Res 2004;83:849-53.
14. Ab Llah N, Jamaludin SB, Daud ZC, Zaludin MAF, Jamal ZAZ, Idris MS, et al. Corrosion behavior of Mg-3Zn/bioglass (45S5) composite in simulated body fluid (SBF) and phosphate buffered saline (PBS) solution. AIP Conf Proc 2016;1756:030001-7.
15. Zoergiebel J, Ilie N. An in vitro study on the maturation of conventional glass ionomer cements and their interface to dentin. Acta Biomater 2013;9:9529-37.
16. Cattani-Lorente MA, Godin C, Meyer JM. Mechanical behavior of glass ionomer cements affected by long-term storage in water. Dent Mater 1994;10:37-44.
17. Ellakuria J, Triana R, Mínguez N, Soler I, Ibaseta G, Maza J, et al. Effect of one-year water storage on the surface microhardness of resin-modified versus conventional glass-ionomer cements. Dent Mater 2003;19:286-90.
18. Wilson AD, Paddon JM, Crisp. The hydration of dental cements. J Dent Res 1979;58:1065-71.
19. Crisp S, Lewis BG, Wilson AD. Characterization of glass-ionomer cements. 1. Long term hardness and compressive strength. J Dent 1976;4:162-6.
20. Pires R, Nunes TG, Abrahams I, Hawkes GE, Morais CM, Fernandez C. Stray-field imaging and multinuclear magnetic resonance spectroscopy studies on the setting of a commercial glass-ionomer cement. J Mater Sci Mater Med 2004;15:201-8.
21. Zainuddin N, Karpukhina N, Hill RG, Law RV. A long-term study on the setting reaction of glass ionomer cements by (27)Al MAS-NMR spectroscopy. Dent Mater 2009;25:290-5.
22. Mesquita MF, Domitti SS, Consani S, de Goes MF. Effect of storage and acid etching on the tensile bond strength of composite resins to glass ionomer cement. Braz Dent J 1999;10:5-9.

23. Tzanakakis E-GC, Tzoutzas IG, Koidis PT. Is there a potential for durable adhesion to zirconia restorations? A systematic review. J Prosthet Dent 2016;115:9-19.
24. Valentino TA, Borges GA, Borges LH, Platt JA, Correr-Sobrinho L. Influence of glazed zirconia on dual-cure luting agent bond strength. Oper Dent 2012;37:181-7.
25. Gomes AL, Castillo-Oyagüe R, Lynch CD, Montero J, Albaladejo A. Influence of sandblasting granulometry and resin cement composition on microtensile bond strength to zirconia ceramic for dental prosthetic frameworks. J Dent 2013;41:31-41.
26. Özcan M, Nijhuis H, Valandro LF. Effect of various surface conditioning methods on the adhesion of dual-cure resin cement with MDP functional monomer to zirconia after thermal aging. Dent Mater J 2008;27:99-104.
27. de Castro HL, Corazza PH, Paes-Júnior Tde A, Della Bona A. Influence of Y-TZP ceramic treatment and different resin cements on bond strength to dentin. Dent Mater 2012;28:1191-7.
28. Özcan M, Bernasconi M. Adhesion to zirconia used for dental restorations: a systematic review and meta-analysis. J Adhes Dent 2015;17:7-26.
29. Matinlinna JP, Heikkinen T, Ozcan M, Lassila LV, Vallittu PK. Evaluation of resin adhesion to zirconia ceramic using some organosilanes. Dent Mater 2006;22:824-31.
30. Özcan M, Vallittu P. Effect of surface conditioning methods on the bond strength of luting cement to ceramics. Dent Mater 2003;19:725-31.
31. Abi-Rached FO, Martins SB, Campos JA, Fonseca RG. Evaluation of roughness, wettability, and morphology of an yttria-stabilized tetragonal zirconia polycrystal ceramic after different airborne-particle abrasion protocols. J Prosthet Dent 2014;112:1385-91.
32. Cotič J, Jevnikar P, Kocjan A. Ageing kinetics and strength of airborne-particle abraded 3Y-TZP ceramics. Dent Mater 2017;33:847-56.
33. Garcia Fonseca R, de Oliveira Abi-Rached F, dos Santos Nunes Reis JM. Effect of particle size on the flexural strength and phase transformation of an airborne-particle abraded yttria-stabilized tetragonal zirconia polycrystal ceramic. J Prosthet Dent 2013;110:510-4.
34. Ozcan M, Melo RM, Souza RO, Machado JP, Felipe Valandro L, Botttino MA. Effect of air-particle abrasion protocols on the biaxial flexural strength, surface characteristics and phase transformation of zirconia after cyclic loading. J Mech Behav Biomed Mater 2013;20:19-28.
35. Souza RO, Valandro LF, Melo RM, Machado JP, Bottino MA, Ozcan M. Air-particle abrasion on zirconia ceramic using different protocols: effects on biaxial flexural strength after cyclic loading, phase transformation and surface topography. J Mech Behav Biomed Mater 2013;26:155-63.
36. Wang H, Aboushelib MN, Feilzer AJ. Strength influencing variables on CAD/CAM zirconia frameworks. Dent Mater 2008;24:633-8.
37. DeHoff PH, Anusavice KJ, Wang Z. Three-dimensional finite element analysis of the shear bond test. Dent Mater 1995;11:126-31.
38. Armstrong S, Geraldeli S, Maia R, Raposo LH, Soares CJ, Yamagawa J. Adhesion to tooth structure: a critical review of "micro" bond strength test methods. Dent Mater 2010;26:e50-62.
39. Altintas S, Eldeniz AU, Usumez A. Shear bond strength of four resin cements used to lute ceramic core material to human dentin. J Prosthodont 2008;17:634-40.
40. Turkun M, Cal E, Toman M, Toksavul S. Effects of dentin disinfectants on the shear bond strength of all-ceramics to dentin. Oper Dent 2005;30:453-60.
41. Erdemir U, Sancakli HS, Sancakli E, Eren MM, Ozel S, Yucel T, et al. Shear bond strength of a new self-adhering flowable composite resin for lithium disilicate-reinforced CAD/CAM ceramic material. J Adv Prosthodont 2014;6:434-43.
42. Komsta L. Processing data for outliers. R News 2006;6:10-3.
43. Dixon WJ. Analysis of extreme values. Ann Math Stat 1950;21:488-506.
44. Dixon WJ. Ratios involving extreme values. Ann Math Stat 1951;22:68-78.
45. Rorabacher DB. Statistical treatment for rejection of deviant values: critical values of dixon q parameter and related subrange ratios at the 95 percent confidence level. Anal Chem 1991;83:139-46.
46. Grubbs FE. Sample criteria for testing outlying observations. Ann Math Stat 1950;21:27-58.
47. IBM Corp. IBM SPSS Statistics for Windows, Version 21.0. Armonk, NY: IBM Corp; 2012.
48. Oyane A, Kim H-M, Furuya T, Kokubo T, Miyazaki T, Nakamura T. Preparation and assessment of revised simulated body fluids. J Biomed Mater Res 2003;65:188-95.
49. de Oliveira IR, Raniero LJ, Leite VMC, Castro-Raucci LMS, de Oliveira PT, Pandolfelli VC. In vitro apatite-forming ability of calcium aluminate blends. Ceram Int 2017;43:10071-9.
50. Torréns-Martín D, Fernández-Carrasco L, Martínez-Ramírez S. Hydration of calcium aluminates and calcium sulfoaluminate studied by Raman spectroscopy. Cem Concr Res 2013;47:43-50.
51. Kirwan LJ, Fawell PD, Van Bronswijk W. In situ FTIR-ATR examination of poly(acrylic acid) adsorbed onto hematite at low pH. Langmuir 2003;19:5802-7.
52. Grabowska B, Holtzer M. Structural examination of the cross-linking reaction mechanism of polyacrylate binding agents. Arch Metall Mater 2009;54:427-37.
53. Kirwan LJ, Fawell PD, Van Bronswijk W. An in situ FTIR-ATR study of polyacrylate adsorbed onto hematite at high pH and high ionic strength. Langmuir 2004;20:4093-100.
54. Bosomworth DR. Far-infrared optical properties of CaF_2, SrF_2, BaF_2, and CdF_2. Phys Rev 1967;157:709-15.
55. Cullity BD. Elements of X-Ray Diffraction. 2nd ed. Chicago, Illinois: Addison-Wesley Publishing Company Inc; 1978. p. 81-99.
56. Voll D, Lengauer C, Beran A, Schneider H. Infrared band assignment and structural refinement of Al–Si, Al–Ge, and Ga–Ge mullites. Eur J Mineral 2001;13:591-601.

Corresponding author:
Dr Petros Koidis
Laboratory of Prosthodontics
Department of Dentistry
Aristotle University of Thessaloniki
University Campus, Dentistry Building
GR 54124
Thessaloniki
GREECE
Email: pkoidis@dent.auth.gr

Acknowledgments
The authors wish to thank mathematician Dr Vasilios Karagiannis for the statistical analysis; PhD Candidate Miss Lambrini Malletzidou for performing the XRD measurements; and dental technician Nikolaos Nikoloudias for milling the specimens. The experimental procedures (SBS test) were performed at the Department of Basic Dental Sciences, Division of Dental Tissues Pathology and Therapeutics, School of Dentistry, Faculty of Health Sciences, Aristotle University of Thessaloniki, Greece, with the assistance of Dr Alexandros Nikolaidis.

Copyright © 2019 by the Editorial Council for *The Journal of Prosthetic Dentistry*.

https://doi.org/10.1016/j.prosdent.2019.04.016